

# Oxygen adatoms at SrTiO<sub>3</sub>(001): A density-functional theory study

Hannes Guhl,<sup>1,2</sup> Wolfram Miller,<sup>3</sup> and Karsten Reuter<sup>1</sup>

<sup>1</sup>*Fritz-Haber-Institut der Max-Planck-Gesellschaft, Faradayweg 4-6, D-14195 Berlin, Germany*

<sup>2</sup>*Leibniz Institut für Kristallzüchtung, Max-Born-Str. 2, D-12489 Berlin, Germany*

<sup>3</sup>*Institut für Kristallzüchtung, Max-Born-Str. 2, D-12489 Berlin, Germany*

(Received July 15, 2009)

We present a density-functional theory study addressing the energetics and electronic structure properties of isolated oxygen adatoms at the SrTiO<sub>3</sub>(001) surface. Together with a surface lattice oxygen atom, the adsorbate is found to form a peroxide-type molecular species. This gives rise to a non-trivial topology of the potential energy surface for lateral adatom motion, with the most stable adsorption site not corresponding to the one expected from a continuation of the perovskite lattice. With computed modest diffusion barriers below 1 eV, it is rather the overall too weak binding at both regular SrTiO<sub>3</sub>(001) terminations that could be a critical factor for oxide film growth applications.

## I. INTRODUCTION

Apart from its use in photo-catalytic and sensing applications<sup>1,2</sup>, the SrTiO<sub>3</sub>(001) surface is also receiving increasing attention as a suitable substrate material for thin film growth<sup>3,4</sup>. For the latter context the numerous reported surface reconstructions<sup>5,6,7,8,9,10,11,12</sup>, partly in sensitive dependence of the applied annealing temperature, indicate a complex surface kinetics, which needs to be understood and controlled when aiming at growth experiments tailored to the atomic-scale. This view of the surface being far from equilibrium under the employed experimental conditions<sup>12,13</sup> is corroborated by first-principles thermodynamic calculations<sup>13,14,15</sup>, which identified the unreconstructed surface as the only equilibrium termination. In the resulting focus on the adsorption kinetics, a first important step is to establish detailed insight into the nature of the bond and the concomitant binding and diffusion properties of all surface species involved. Studying the interaction of oxygen with SrTiO<sub>3</sub>(001) is in this respect a natural starting point, in light of the important role played by oxygen exposure for surface preparation and growth or gas-sensing applications. Seemingly simple at first glance, preceding experimental and theoretical work has already revealed intriguing aspects even of the initial surface intermediates. Not untypical for wide band-gap oxides<sup>3,16</sup>, spectroscopic and kinetic investigations suggest the existence of a molecular peroxide “O<sub>2</sub><sup>-2</sup>” species at the surface<sup>17,18</sup>. This is confirmed by recent density-functional theory (DFT) calculations by Piskunov *et al.*<sup>19</sup>, which demonstrate that this peroxide species results at both regular SrTiO<sub>3</sub>(001) terminations actually from the bonding of an O adatom to a surface O ion of the oxide lattice.

The formation of such a dioxygen moiety may readily give rise to a non-trivial topology of the potential energy surface (PES) for lateral diffusion of adsorbed O atoms across the surface, with direct consequences for the role of O adatoms in the growth kinetics. Aiming to elucidate the latter we therefore employ DFT to explicitly map this PES for isolated O adatoms at both regular SrTiO<sub>3</sub>(001) terminations and discuss the impli-

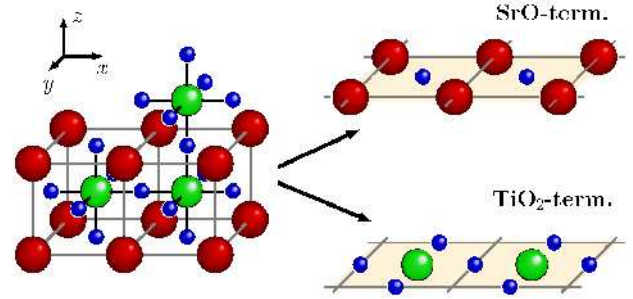


FIG. 1: (Color online) Schematic illustration of the crystal structure of cubic SrTiO<sub>3</sub> and its two regular (001) terminations, featuring a TiO<sub>2</sub> or SrO composition in the topmost layer. O atoms are depicted as small, light gray (blue) spheres, Ti atoms as medium-size, gray (green) spheres and Sr atoms as large, dark (red) spheres.

cations of the obtained energetic data with respect to the presence and mobility of this surface species. The computed surface electronic structure indeed suggests that the complex formed between the O adatom and lattice oxygen ion may be characterized as a molecular peroxide species. While this surface bond is at both terminations strong enough to shift the most stable adsorption site away from the one that would correspond to a continuation of the perovskite lattice, the absolute bond strength is only about the same as in gas-phase O<sub>2</sub> and the diffusion barrier with 0.8 eV quite modest. This points to the overall stabilization, rather than the mobility of a corresponding O adatom species as critical factor for the growth kinetics at this surface.

## II. THEORY

Identified as the only equilibrium surface structures<sup>13,14,15</sup>, the regular TiO<sub>2</sub>- and SrO-terminations illustrated in Fig. 1 form a natural basis for our fundamental study addressing the energetics and

electronic structure of O adatoms at cubic SrTiO<sub>3</sub>(001). All corresponding DFT calculations were performed with the CASTEP<sup>20</sup> code using a plane-wave basis together with ultrasoft pseudopotentials<sup>21</sup> as provided in the default library, and the GGA-PBE functional<sup>22</sup> to treat electronic exchange and correlation (xc). Tests using the LDA did not yield any qualitative differences with respect to the conclusions put forward below. The surfaces were modeled with supercell geometries, using inversion-symmetric slabs based on the GGA-PBE optimized bulk lattice constant ( $a_0 = 3.938 \text{ \AA}$ ), with O adsorption at both sides and with a vacuum separation exceeding 13 Å. Apart from the central three layers of the slab, all substrate atomic positions were fully relaxed until the absolute value of all ionic forces dropped below 0.1 eV/Å, with further tightening of this criterion not yielding any significant changes with respect to surface geometry and concomitant energetics. This relaxation was equally applied to the  $z$ -height of the O adatom, with its  $x$  and  $y$  coordinates frozen at different positions to map the PES for lateral adatom motion.

The centrally targeted energetic quantity is the binding energy of an O adsorbate, defined as

$$E_b = \frac{1}{2} [E_{\text{O@surf}} - E_{\text{surf}} - E_{\text{O}_2(\text{gas})}] \quad , \quad (1)$$

where  $E_{\text{O@surf}}$  is the total energy of the O covered surface,  $E_{\text{surf}}$  the total energy of the clean surface,  $E_{\text{O}_2(\text{gas})}$  the total energy of the gas-phase O<sub>2</sub> molecule (all three computed at the same plane-wave cutoff), and the factor 1/2 accounts for the fact that adsorption is at both sides of the slab. The binding energy is thus referenced to a free O<sub>2</sub> molecule in its spin-triplet ground state (calculated in a  $(18 \times 18 \times 18) \text{ \AA}$  supercell), and a negative value of  $E_b$  indicates that adsorption is exothermic. Both  $E_{\text{O@surf}}$  and  $E_{\text{surf}}$  were furthermore consistently computed in a non spin-polarized way, with systematic tests confirming that spin-polarization at the surface does not play any significant role for the description of all relevant low-energy parts of the PES.

Systematic tests with one O adatom at different high-symmetry sites in a  $(1 \times 1)$  surface unit-cell verified that  $E_b$  is numerically converged with respect to the basis set to within  $\pm 20 \text{ meV}$  when employing a plane wave kinetic energy cutoff of 430 eV. Due to long-range geometric relaxations<sup>24</sup> achieving a similar convergence with respect to the number of surface unit cells in the slab model is more challenging. This concerns prominently those adsorption sites where the O adatom protrudes significantly from the surface, e.g. on-top of the lattice Ti-atom on the TiO<sub>2</sub> termination. However, at the same time such sites are energetically so unfavorable that they do not even belong to the saddle point regions of the adatom PES that are relevant for the diffusion barriers. Consequently, we employed  $(3 \times 3)$  surface unit-cells with a  $(2 \times 2 \times 1)$  Monkhorst-Pack grid<sup>23</sup> for the reciprocal space integrations. Test calculations in larger surface unit-cells indicate that this set-up provides a very good description

of the isolated adatom limit with respect to the most stable site and diffusion barriers addressed here. The slab models comprised in total seven and 11 atomic layers for the TiO<sub>2</sub>- and SrO-termination, respectively, which ensure that all energetically relevant parts of the adatom PES discussed below are converged to at least within  $\pm 50 \text{ meV}$ .

### III. RESULTS

#### A. Geometric structure and energetics

Figure 2 summarizes the computed PES for lateral O adatom motion at both regular terminations. As suspected, the shape is in both cases non-trivial, with the global minimum, i.e. most stable adsorption site, not corresponding to the one expected from a mere continuation of the perovskite lattice. The geometric adsorption structure at this most stable site shown in Fig. 3 for both terminations is indeed very consistent with the anticipated reason<sup>19</sup> for this PES topology in form of strong bonding between the adsorbate and a SrTiO<sub>3</sub>(001) surface oxygen anion (*vide infra*). At the SrO-termination this directly coordinated lattice oxygen atom is pulled out of the surface while the underlying Ti atom, denoted as Ti(1) in Fig. 3, is pressed into the bulk material, thereby stretching the Ti-O bond from 1.97 Å to 2.20 Å.

On the other hand the distance to the adsorbed O<sub>ad</sub> atom is quite short, and with 1.52 Å rather characteristic for a molecular peroxide “O<sub>2</sub><sup>-2</sup>” species<sup>3,16</sup>. With respect to the surface normal the dioxygen complex is tilted with a Ti(1)-O-O<sub>ad</sub> angle of 120° and points between two surface Sr atoms. However, the barrier for a 90° rotation of the complex around the  $z$ -axis to point between an adjacent pair of Sr atoms is only 0.24 eV, cf. Fig. 2. One could thus view the dioxygen moiety as a tilted, singly-bonded  $\eta^1$  “end-on” configuration with respect to the underlying Ti(1) cation in the second layer, with the tilt direction exhibiting some dynamics at finite temperature.

At the TiO<sub>2</sub>-termination only atoms in the topmost layer are significantly affected by the presence of the oxygen adatom. The oxygen-oxygen bond measures 1.47 Å and is therewith again in the ballpark expected for a molecular peroxide species. It is tilted towards one of the adjacent Ti surface atoms denoted as Ti(1) in Fig. 3, such that the distance between O<sub>ad</sub> and the latter is 1.91 Å and the Ti(1)-O-O<sub>ad</sub> tilt angle is 62°. This geometry is thus more reminiscent of an asymmetric, doubly-bonded  $\eta^2$  “side-on” configuration with respect to the coordinated Ti(1) cation, which is in fact the more usual form in dioxygen-Ti complexes<sup>25</sup> and with the respective bond-lengths and angles of the Ti(1)-O-O<sub>ad</sub> moiety agreeing again specifically with those of peroxotitanium complexes<sup>26</sup>. Despite this coordination a flipping motion of the dioxygen moiety to the adjacent Ti atom denoted as Ti(2) in Fig. 3 has only a small computed barrier of

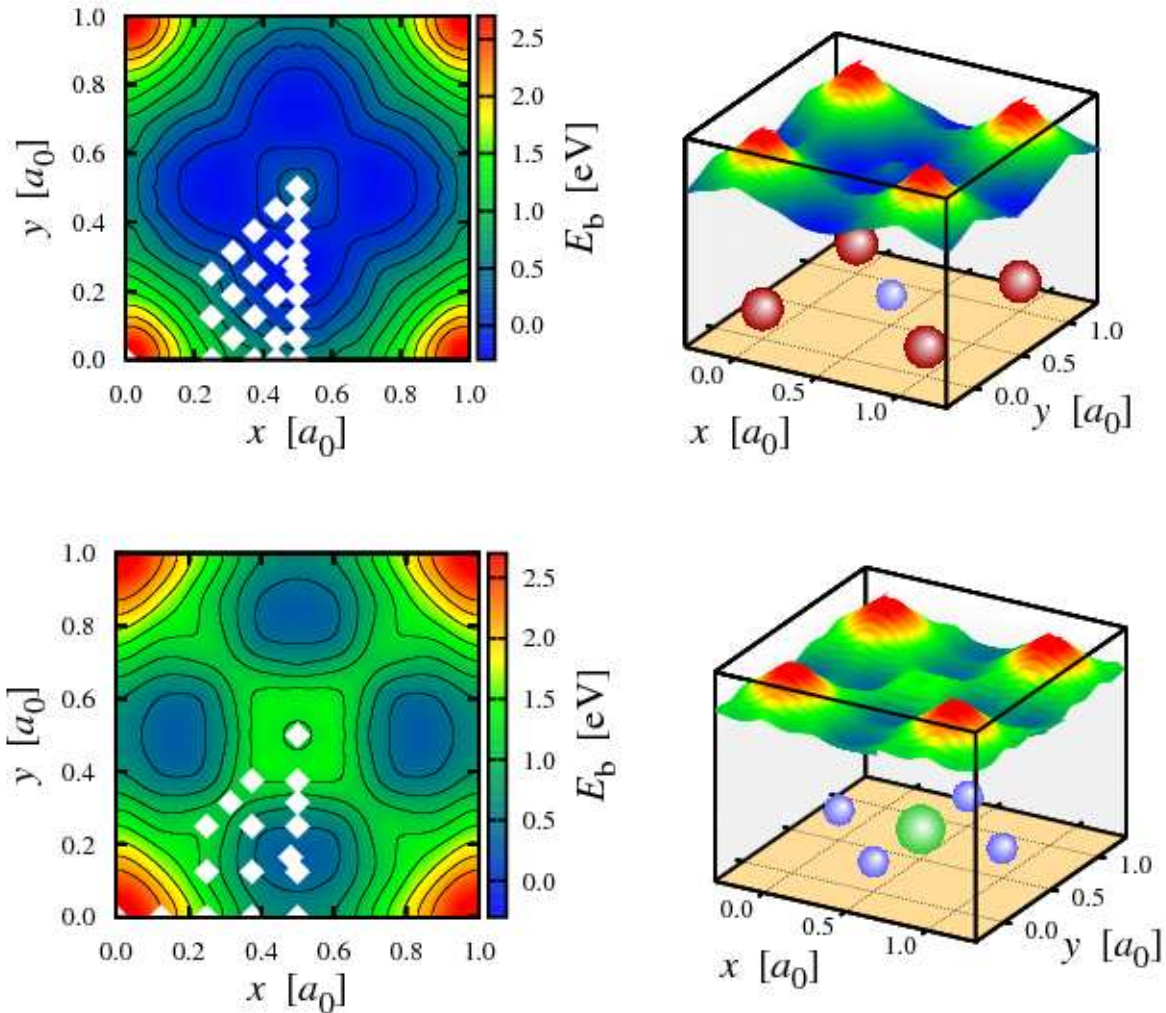


FIG. 2: (Color online) Potential energy surface  $PES(x,y)$  for lateral motion of an O adatom at the SrO- and  $TiO_2$ -termination, upper and lower panels respectively. The lateral coordinates  $x$  and  $y$  are given in units of the bulk lattice constant  $a_0 = 3.938 \text{ \AA}$ , with the shown range for each termination exactly corresponding to the surface unit-cell definition shown in Fig. 1. At the SrO-termination, the position  $(0,0)$  is thus directly atop a surface Sr atom, while at the  $TiO_2$ -termination the position  $(1/2, 1/2)$  is atop a surface Ti atom. The white diamonds denote the actually calculated points within the irreducible wedge and neighboring isolines correspond to a difference of  $0.25 \text{ eV}$ .

$0.30 \text{ eV}$  as shown in Fig. 2, which again indicates some dangling dynamics at finite temperature.

Even in this most stable site at the  $TiO_2$ -termination the computed binding energy is with  $0.30 \text{ eV}$  still endothermic with respect to gas-phase  $O_2$ . However, due to the known shortcomings of the employed gradient-corrected xc functional such absolute binding energy values have to be considered with care. In this respect, it is quite gratifying that the preceding study by Piskunov and coworkers<sup>19</sup>, which employed a hybrid functional including some non-local Hartree-Fock exchange, reports a rather similar binding energy of  $0.66 \text{ eV}$  at the same most stable site and with nearly identical geometry parameters. In fact, when redoing our calculations in the smaller

$(2 \times 2)$  surface unit-cell employed by them we arrive at a virtually coinciding  $E_b = 0.60 \text{ eV}$ . This seems to indicate that a proper account of the long-range geometric relaxations enabled in the larger surface unit-cells accessible with the computationally much less demanding semi-local functional have a larger effect on the binding energetics than the improved xc description introduced by the hybrid functional. Furthermore, we believe that the additional GGA advantage of being able to perform a much more thorough exploration of the PES has direct consequences for the comparison of the results obtained for the SrO-termination. Within the understanding of the PES topology shown in Fig. 2 it appears as if the restricted testing of three possible high-symmetry adsorption sites

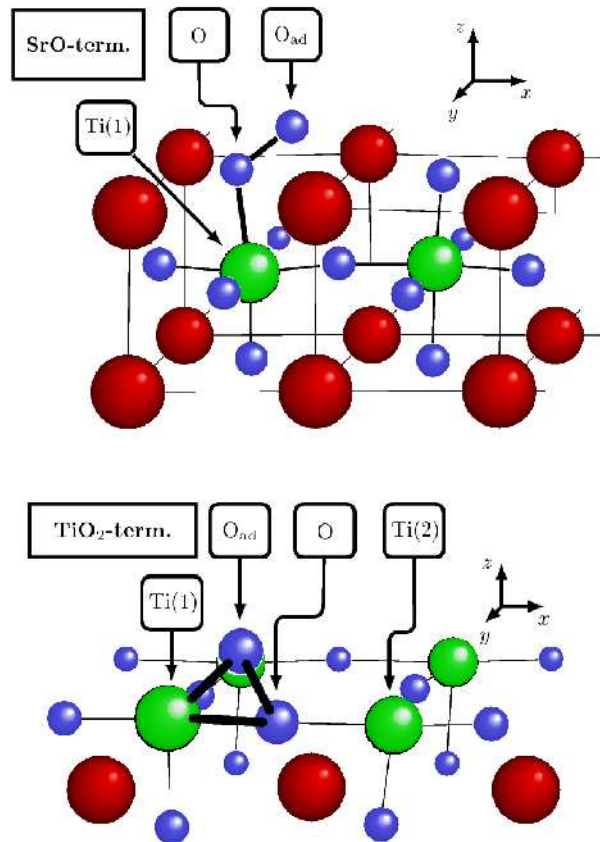


FIG. 3: (Color online) Perspective view of the most stable O adsorption geometry at the SrO- and TiO<sub>2</sub>-termination, upper and lower panel respectively. Atoms specifically referred to in the text are labeled. O atoms are depicted as small, light gray (blue) spheres, Ti atoms as medium-size, gray (green) spheres and Sr atoms as large, dark (red) spheres.

has misled the authors of ref.<sup>19</sup> to erroneously identify the transition-state for the rotational motion of the oxygen moiety around the  $z$ -axis as most stable adsorption site, while the PES area around the above described most stable site of lower symmetry was not scanned in their study. Recomputing this transition state in the smaller surface unit-cell we again achieve excellent agreement between our GGA-PBE and their reported hybrid functional energetics, which fortifies our confidence in the here calculated slightly exothermic  $E_b = -0.20$  eV at the most stable site shown in Fig. 3.

At least at the TiO<sub>2</sub>-termination the binding is thus clearly too weak to generate O adatoms through dissociative adsorption at the ideal terraces. This is commonly expected for insulating oxides<sup>3</sup> and has been verified explicitly for related materials like SnO<sub>2</sub><sup>27</sup>, MgO<sup>28</sup> and TiO<sub>2</sub><sup>29</sup>. Considering the high vacancy formation energies<sup>24</sup>, it would, however, energetically clearly be

possible to create an O adatom by adsorbing an oxygen molecule into a surface O vacancy at both regular terminations. Once established at the surface, the computed barriers for diffusive motion to the adjacent binding site of 0.81 eV and 0.68 eV at the SrO- and TiO<sub>2</sub>-termination respectively, cf. Fig. 2, demonstrate that the O-O<sub>ad</sub> bond is then much more readily broken compared to the desorption of the O-O<sub>ad</sub> molecule so that O adatoms should be a relatively mobile species.

## B. Electronic structure

The preceding section has discussed the geometric structure and adsorption energetics within the picture of a quasi-molecular species formed between the O adatom and a directly coordinated lattice O anion. This view is nicely supported by the adsorbate-induced change of the electron density shown in Fig. 4. This quantity, commonly referred to as “difference electron density”<sup>30</sup>, is obtained by subtracting from the electron density of the O@SrTiO<sub>3</sub>(001) system both the electron density of the clean SrTiO<sub>3</sub>(001) surface and that of an isolated oxygen atom. Here, the atomic positions of SrTiO<sub>3</sub>(001) and of the O atom are taken to be same as those of the relaxed adsorbate system. In this way, the presentation highlights the charge rearrangement upon bond formation, which as clear from Fig. 4 primarily takes place between the O adatom and its lattice O partner.

Some further quantification of this adsorbate-induced charge redistribution can be obtained from an inspection of the Mulliken<sup>31</sup> and Hirshfeld<sup>32</sup> charges on the various surface species. With the two charge partitioning schemes yielding the usual differences in absolute numbers, they nevertheless unanimously predict the same trend in that the charge surplus at the lattice O anion is essentially evenly distributed over the formed dioxygen moiety after adsorption. In other words, while the charges on all other atoms in the topmost two layers are virtually unaffected by the adsorbed O atom, the charge on the directly coordinated lattice O anion gets about halved with the O adatom exhibiting a charge of roughly equal magnitude. For the Mulliken (Hirshfeld) scheme this means specifically that at the TiO<sub>2</sub>-termination the computed charge of  $-0.73e$  ( $-0.33e$ ) at the surface O anion, diminishes to  $-0.49e$  ( $-0.16e$ ) upon adsorption with the O adatom exhibiting a similar charge of  $-0.38e$  ( $-0.16e$ ). At the SrO-termination the equivalent numbers are  $-0.83e$  ( $-0.38e$ ) and  $-0.54e$  ( $-0.20e$ ) for the surface anion before and after O adsorption, as well as  $-0.58e$  ( $-0.30e$ ) for the O adatom. The thereby suggested formation of a molecular peroxide “O<sub>2</sub><sup>-2</sup>” species is corroborated by an analysis of the density of states (DOS) at the surface, which we focus for the present purposes on the O  $2s$  dominated states around 20 eV below the bulk valence band maximum. Figure 5 compiles the corresponding calculations and compares them to the oxygen-projected DOS of bulk SrO<sub>2</sub>, a material in which



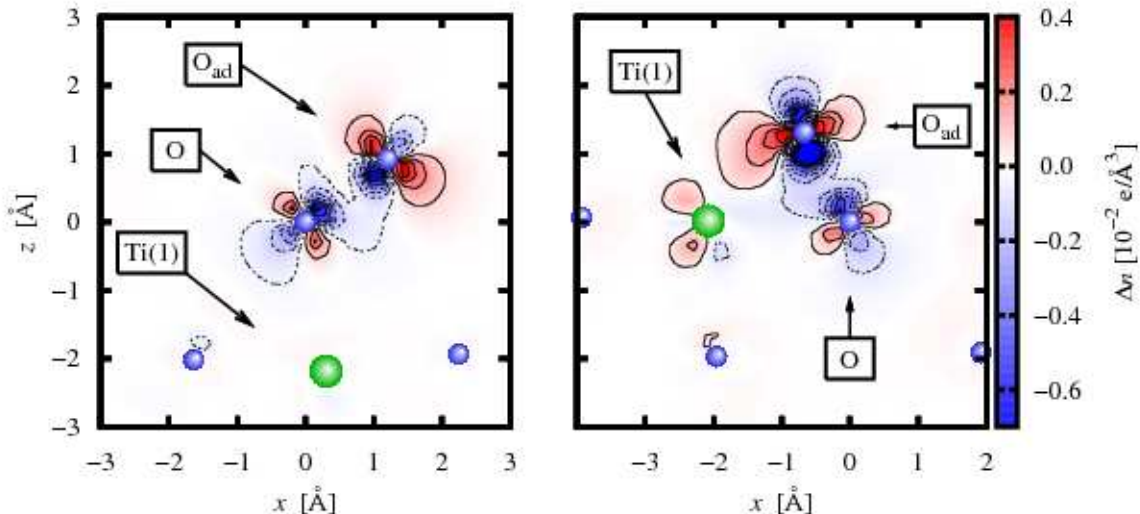


FIG. 4: (Color online) Difference electron density  $\Delta n(\mathbf{r})$  plot highlighting the formation of a dioxygen moiety at the SrO- and TiO<sub>2</sub>-termination, left and right panel respectively. Shown is the charge rearrangement within the plane perpendicular to the surface defined by the O<sub>ad</sub> adatom and its directly coordinated lattice O and Ti(1) partners, cf. Fig. 3, with red (blue) areas with solid (dashed) contour lines depicting charge depletion and accumulation, respectively. Neighboring isolines indicate a difference of  $10^{-3}e/\text{\AA}^3$ . The superimposed spheres indicate the position of atoms within the plane, using the color and size scheme for the individual species as in Figs. 1 and 3.

O<sub>2</sub><sup>-2</sup>-type bonding occurs naturally. Apparently, O adsorption at SrTiO<sub>3</sub>(001) leads at both terminations to two sharp fingerprint states above and below the regular SrTiO<sub>3</sub> O 2s group, which almost perfectly match the energetic position of the equivalent states in bulk SrO<sub>2</sub>. This confirms the interpretation in terms of a molecular peroxide species, the bond of which leads to the non-trivial PES topology for O adatom diffusion described in Section 3.A.

#### IV. CONCLUSIONS

In conclusion we have presented a density-functional theory study analyzing the potential-energy surface for lateral diffusion of O adatoms at both regular terminations of SrTiO<sub>3</sub>(001). The O adatom is found to form a quasi-molecular “O<sub>2</sub><sup>-2</sup>”-type species with a directly coordinated surface O anion of the substrate lattice. This bond is strong enough to shift the most stable adsorption site away from the one expected from a mere continuation of the perovskite lattice, and gives rise to a non-trivial PES topology that allows for some dangling dynamics of the dioxygen moiety at finite temperature. In addition, the computed barriers for diffusive hops to adjacent binding sites are at both terminations well below 1 eV, so that mobility of O adatoms is not expected to represent a bottleneck at typical film growth conditions. On the

other hand, the overall bond strength is at both terminations only about equal to the one of a O<sub>2</sub> molecule, and specifically slightly exothermic at the SrO-termination and slightly endothermic at the TiO<sub>2</sub>-termination with respect to this gas-phase reference. At least at the latter termination the binding is thus clearly too weak to generate O adatoms through dissociative adsorption at ideal SrTiO<sub>3</sub>(001) terraces. In view of the high O surface vacancy formation energies, an at least energetically much more plausible alternative would be that O adatoms are created by adsorbing an oxygen molecule into such a defect. Once established at the surface, the computed modest diffusion barriers show that the “O<sub>2</sub><sup>-2</sup>” peroxide-type bond is broken rather readily, suggesting that such O adatoms would provide a mobile species that could anneal further defects or attach to created islands.

#### Acknowledgements

All calculations have been performed on the SGI Altix ICE- and XE- computing clusters of the North-German Supercomputing Alliance (HLRN) hosted at Konrad-Zuse-Zentrum für Informationstechnik in Berlin (ZIB) and at Regionales Rechenzentrum für Niedersachsen (RRZN) at Leibniz Universität Hannover. We are particularly grateful to B. Kallies for technical support.

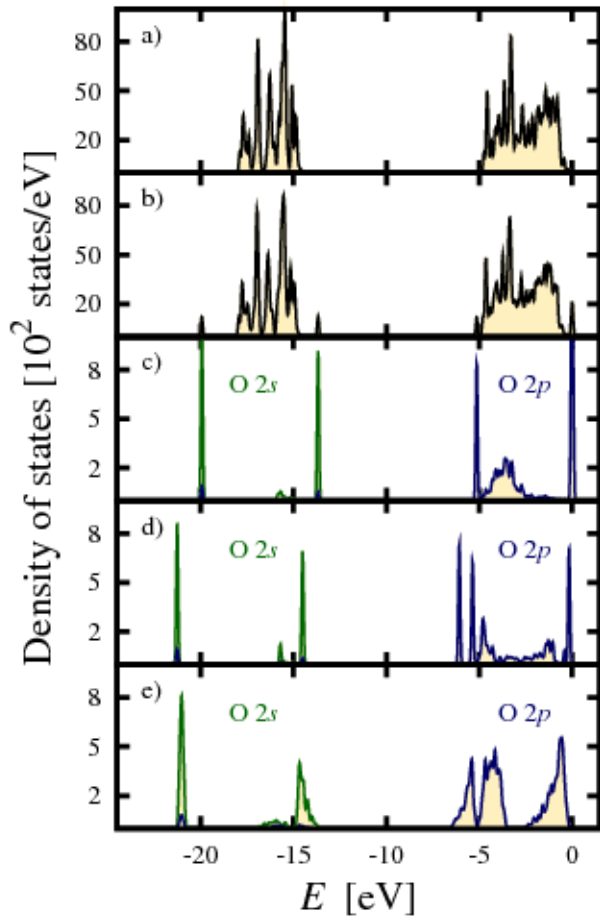


FIG. 5: (Color online) Density of states (DOS) analysis supporting the interpretation of the formed  $O_{ad}$ -O complex in terms of a molecular peroxide species. The topmost panels show the total DOS of the topmost two surface layers of the SrO-termination of clean SrTiO<sub>3</sub>(001) before (a) and after (b) O adsorption. The next two panels show the DOS projected onto the  $2s$  (green line) and  $2p$  (blue line) states of the  $O_{ad}$  atom and its coordinated lattice O partner for the SrO- (c) and the TiO<sub>2</sub>-termination (d), identifying in particular two sharp states above and below the O  $2s$  group as fingerprints for the formed  $O_{ad}$ -O moiety. Panel (e) shows the same projected DOS of bulk SrO<sub>2</sub> exhibiting essentially the same characteristics. The bulk valence band maximum (as approximately reached in the central slab layer) is taken as zero reference in all panels.

<sup>1</sup> J.G. Mavroides, J.A. Kafalas, and D.F. Kolesar, Appl. Phys. Lett. **28**, 241 (1976).  
<sup>2</sup> R. Merkle and J. Maier, Angew. Chem. Int. Ed. **47**, 3874 (2008).  
<sup>3</sup> V.E. Henrich and P.A. Cox, *The Surface Science of Metal Oxides*, Cambridge University Press, Cambridge (1994)  
<sup>4</sup> V.C. Matijasevic, B. Ilge, B. Stäuble-Pümpin, G. Rietveld, F. Tuinstra, and J.E. Mooij, Phys. Rev. Lett. **76**, 4765

(1996).  
<sup>5</sup> Y. Liang and D.A. Bonnell, Surf. Sci. **310**, 128 (1994).  
<sup>6</sup> M. Naito and H. Sato, Physica C **229**, 1 (1994).  
<sup>7</sup> K. Szot and W. Speier, Phys. Rev. B **60**, 5909 (1999).  
<sup>8</sup> T. Kubo and H. Nozoye, Phys. Rev. Lett. **86**, 1801 (2001).  
<sup>9</sup> N. Erdman, K.R. Poeppelmeier, M. Asta, O. Warschkow, L.D. Marks, and D.E. Ellis, Nature **419**, 55 (2002).  
<sup>10</sup> V. Vonk, S. Konings, G. van Hummel, S. Harkema, and H.

- Graafsma, Surf. Sci. **595**, 183 (2005).
- <sup>11</sup> C.H. Lanier, A. van de Walle, N. Erdman, E. Landree, O. Warschkow, A. Kazimirov, K.R. Poepelmeier, J. Zegenhagen, M. Asta, and L.D. Marks, Phys. Rev. B **76**, 045421 (2007).
- <sup>12</sup> R. Heger, P.R. Willmott, O. Bunk, C.M. Schlepütz, B.D. Patterson, B. Delley, V.L. Shneerson, P.F. Lyman, and D.K. Saldin, Phys. Rev. B **76**, 195435 (2007).
- <sup>13</sup> L.M. Liborio, C.G. Sanchez, A.T. Paxton, and M.W. Finnis, J. Phys.: Condens. Matter **17**, L223 (2005).
- <sup>14</sup> K. Johnston, M.R. Castell, A.T. Paxton, and M.W. Finnis, Phys. Rev. B **70**, 085415 (2004).
- <sup>15</sup> E. Heifets, S. Piskunov, E.A. Kotomin, Y.F. Zhukovskii, and D.E. Ellis, Phys. Rev. B **75**, 115417 (2007).
- <sup>16</sup> M. Che and A.J. Trench, Adv. Catal. **32**, 1 (1983).
- <sup>17</sup> V.M. Bermudez and V.H. Ritz, Chem. Phys. Lett. **73**, 160 (1980).
- <sup>18</sup> R. Merkle and J. Maier, Phys. Chem. Chem. Phys. **4**, 4140 (2002).
- <sup>19</sup> S. Piskunov, Y.F. Zhukovskii, E.A. Kotomin, E. Heifets, and D.E. Ellis, Proc. of Mat. Res. Soc. Symposia **894**, 295 (2006).
- <sup>20</sup> S. Clark, M.D. Segall, C.J. Pickard, P.J. Hasnip, M.I.J. Probert, K. Refson, and M.C. Payne, Z. Kristallogr. **220**, 567 (2005).
- <sup>21</sup> D. Vanderbilt, Phys. Rev. B **41**, 7892 (1990).
- <sup>22</sup> J.P. Perdew, K. Burke, and M. Ernzerhof, Phys. Rev. Lett. **77**, 3865 (1996).
- <sup>23</sup> H. Monkhorst and J. Pack, Phys. Rev. B **13**, 5188 (1976).
- <sup>24</sup> J. Carrasco, F. Illas, N. Lopez, E.A. Kotomin, Y.F. Zhukovskii, R.A. Evarestov, Y.A. Mastrikov, S. Piskunov, and J. Maier, Phys. Rev. B **73**, 064106 (2006).
- <sup>25</sup> L. Vaska, Acc. Chem. Res. **9**, 175 (1976).
- <sup>26</sup> D. Schwarzenbach, Inorg. Chem. **9**, 2391 (1970).
- <sup>27</sup> J. Oviedo and M.J. Gillan, Surf. Sci. **490**, 221 (2001).
- <sup>28</sup> L.N. Kantorovich and M.J. Gillan, Surf. Sci. **374**, 373 (1997).
- <sup>29</sup> M.D. Rasmussen, L.M. Molina, and B. Hammer, J. Chem. Phys. **120**, 988 (2004).
- <sup>30</sup> M. Scheffler and C. Stampfl, *Theory of Adsorption on Metal Substrates*, In: Handbook of Surface Science, Vol. **2**: Electronic Structure, (Eds.) K. Horn and M. Scheffler, Elsevier, Amsterdam (2000).
- <sup>31</sup> R.S. Mulliken, J. Chem. Phys. **23**, 1833 (1955).
- <sup>32</sup> F.L. Hirshfeld, Theor. Chim. Acta **44**, 129 (1977).